Materials Science and Engineering A 529 (2011) 215–223

Contents lists available at SciVerse ScienceDirect

Materials Science and Engineering A

journal homepage: www.elsevier.com/locate/msea

Effect of clay organic modifier on the final performance of PCL/clay nanocomposites

L.N. Ludueña [a,1], J.M. Kenny [b], A. Vázquez [c], V.A. Alvarez [a,*]

[a] Research Institute of Material Science and Technology (INTEMA), Engineering Faculty, National University of Mar del Plata, Juan B. Justo 4302 (B7608FDQ), Mar del Plata, Argentina
[b] Institute of Polymers Science and Technology, ICTP, Juan de la Cierva 3, 28006 Madrid, Spain
[c] INTECIN (UBA-CONICET), Polymer and Composite Group, Engineering Faculty, University of Buenos Aires, Las Heras 2214 (C1063ACV), Buenos Aires, Argentina

ARTICLE INFO

Article history:
Received 14 April 2011
Received in revised form 15 August 2011
Accepted 8 September 2011
Available online 16 September 2011

Keywords:
Mechanical characterization
X-ray diffraction
Polymers
Nanostructured materials
Thermomechanical processing

ABSTRACT

The effect of un-modified and several organo-modified montmorillonites on the morphology, mechanical properties and thermal behavior of polycaprolactone (PCL) based nanocomposites prepared by melt intercalation was studied. The study was centered on the analysis of the clay characteristics that have influence on the final properties of PCL/clay nanocomposites. Polymer/clay compatibility was analyzed studying both bulk and surface polarity degree of the clays by means of water absorption tests (bulk) and contact angle measurements (surface). The thermal stability of the clays was analyzed by dynamic thermogravimetrical tests (TGA). The degradation of the clay organo-modifiers during processing was simulated by isothermal TGA. The clay dispersion degree inside the nanocomposites was analyzed by X-ray diffractometry (XRD). The melt rheology was used as a method to compare the dispersion degree of the clay by means of the shear thinning exponent, n_{Rh}. The tensile mechanical properties were measured and theoretically analyzed by means of several micro-mechanical models. It was found that the thermal stability of the clay organo-modifiers is a critical factor that can modify the final clay content and the clay dispersion degree inside the nanocomposite, demonstrating that the enhancement of the polymer–clay compatibility may not be the main factor to achieve the best mechanical performance when shear forces during processing, i.e. extrusion techniques, are used to prepare polymer/organo-modified clay nanocomposites.

1. Introduction

Because of waste accumulation at the end of the life cycle of traditional polymer products, the development of environmental friendly, degradable, polymeric materials has attracted extensive interest [1]. Polycaprolactone (PCL) is a chemically synthesized polymer based on caprolactone units. It does not occur in nature but it is fully biodegradable [2].

In order to obtain a competitive product, the PCL performance can be greatly enhanced with the addition of nanometer-size inorganic fillers. This kind of materials are called nanocomposites and have the interesting characteristic that the mechanical properties [3]; the barrier properties [4]; the thermal properties [5], and some others such as the flammability [6], water adsorption [7] and creep resistance [8], can be greatly enhanced with the addition of a small amount of filler (usually less than 10 wt.%) [1–8].

One kind of nanometer-size reinforcement is the montmorillonite, which is a layered silicate whose interlayer ions can be exchanged by organ-ions in order to produce an increment in the interlayer spacing (d_{001}) and to improve the polymer/clay compatibility. These improvements allow the dispersion of clay platelets to be easier [9]. Even so, the thermal stability of organic cations is crucial to achieve the highest degree of dispersion [10–20]. In other words, these organic ions can be degraded during the mixing process due to effects of temperature and shear forces, resulting in different trends than those expected. The balance between the compatibility of the components and the thermal stability of organic modifiers will determine the most efficient clay for the matrix used. Xie et al. [10,11] have conducted an extensive review of the processes of degradation of organically modified clays with alkyl ammonium salts. Unfortunately, the temperatures of degradation, yet studied in the absence of shear forces and in non-oxidative atmospheres (thermogravimetric analysis in nitrogen atmosphere), can be reached during the processing of many polymers. This degradation can produce chemical changes and/or physical changes in the structure of the surfactant, and, consequently, can alter the final degree of dispersion of the clay inside the nanocomposite and/or the final interfacial adhesion, which

* Corresponding author. Tel.: +54 223 4816600; fax: +54 223 4810046.
E-mail addresses: luduena@fi.mdp.edu.ar (L.N. Ludueña), avazquez@fi.uba.ar (A. Vázquez), alvarezvera@fi.mdp.edu.ar (V.A. Alvarez).
[1] Tel.: +54 223 4816600; fax: +54 223 4810046.

0921-5093/$ – see front matter © 2011 Elsevier B.V. All rights reserved.
doi:10.1016/j.msea.2011.09.020

Table 1
Characteristics of the clays used as nanofillers.

Clay	Organic modifier	Modifier Concentration (meq/100 g clay)	Specific gravity, ρ_p (g/cm^3)	$d_{0\,0\,1}^{\text{initial}}$ (Å)
Montmorillonite (CNa+)	None	–	2.86	14.0
Cloisite 25A (C25A)	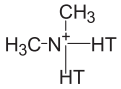	95	1.87	18.6
Closite 30B (C30B)	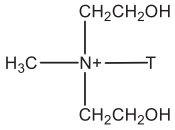	90	1.98	18.8
Closite 10A (C10A)	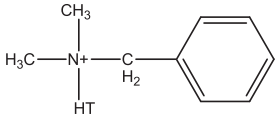	125	1.90	20.0
Cloisite 93A (C93A)	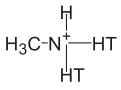	90	1.88	23.6
Cloisite 20A (C20A)	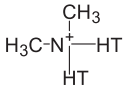	95	1.77	24.2

HT is hydrogenated tallow (∼65% C18; ∼30% C16; ∼5% C14).

influences the physical, mechanical and barrier properties of the nanocomposite obtained [21]. For these reasons, we need a better understanding of the processes of degradation of organic modifiers and how it affects the formation of the nanocomposite.

There have been several investigations about the thermal and mechanical stability of organic modifiers in the preparation of polymer/clay nanocomposites by melt mixing. VanderHart et al. [12,13] have estimated, by testing nuclear magnetic resonance (NMR), that a considerable portion of the alkyl quaternary ammonium compound is removed during the preparation of nylon 6 nanocomposites by melt mixing. They concluded that the main reason of the degradation is the combination of the temperature with shear forces developed during mixing. Moreover, the instability of the organically modified clay can also affect the polymer. Matayabas and Turner [20] have found that degradation occurs in the matrix during the preparation of polyethylene terephthalate nanocomposites with modified clay. Yoon et al. [14] have observed similar effects in the processing of polycarbonate nanocomposites with clays.

Depending on the points discussed above, we conclude that the degree of dispersion achieved in the preparation of nanocomposite polymer/clay depends on several factors: compatibility between components, basal spacing of clay and processing conditions. The conventional way to analyze the best modifier ion for the matrix to be used is to characterize different types of clay and the matrix before and after processing [11–15]. Several studies can be found in the literature regarding PCL/clay nanocomposites [1,3,4,7,21], but it must be taken into account that in order to compare the effect of different organo-modified clays on the final performance of the nanocomposites, they have to be prepared and characterized under same conditions.

The aim of this work was to analyze the effect of clay characteristics (interlaminar space, hidrophilicity and thermal stability) on the morphology, mechanical properties (experimental and modeling) and thermal behavior of polycaprolactone/clay nanocomposites and to use this information in order to determine the best clay for the selected matrix. Isothermal thermogravimetrical analysis was used as a simple method to simulate the degradation of the clay organo-modifiers during mixing that, to our knowledge, was not previously used for this propose. It must be taken into account that the main conclusions of this work can also be extrapolated to other polymer/clay systems as they help to clarify the main responsible factors for the final performance of polymer/clay nanocomposites prepared by melt mixing.

2. Experimental

2.1. Materials

The matrix used in this work was a commercial polycaprolactone (Mn 80,000, $\rho_m = 1.2$ g/cm^3), supplied by Sigma–Aldrich. Several Cloisite clays commercially purchased from Southern Clay Products Inc., USA, were used as nanofillers. They were used as received. The characteristics of the clays are shown in Table 1.

2.2. Nanocomposites preparation

Matrix and nanocomposites with 5 wt.% of each clay, were prepared in a double-screw extruder *DSM Xplore 5&15 microcompounder* using a temperature profile of: 60–90–120 °C at a screw rotating speed of 150 rpm; the residence time was 1 min. Then, films were obtained by compression molding (100 °C, 10 min without pressure and 10 min at 50 bar, mold cooling with water). The different compression molded films were named as PCL for the neat matrix and PCL/CNa+, PCL/C25A, PCL/C30B, PCL/C10A, PCL/C93A, PCL/C20A for the nanocomposites.

2.3. Methods

XRD patterns of clays and nanocomposites were recorded by a PW1710 diffractometer equipped with an X-ray generator ($\lambda = 0.154060$ nm). Samples were scanned in 2θ ranges from 3° to 60° by a step of 0.035°. The interlayer spacing of clays was calculated before and after mixing by means of the *Bragg's Law*. The values were named as $d_{0\,0\,1}^{\text{initial}}$ (before mixing) and $d_{0\,0\,1}^{\text{final}}$ (after mixing).

Contact angle measurements were carried out on the surface of compacts of clay powders that were prepared in a press. Sessile drops of ethylene glycol ($\gamma^d = 30.1$ and $\gamma^p = 17.6$) and diiodomethane ($\gamma^d = 50.8$ and $\gamma^p = 0$) both from Aldrich Co., were formed on the surface of the solids. The contact angles were measured with a Goniometer. Drops dimensions were determined by using the Image Pro-Plus Software. All measurements were carried out at room temperature.

From these measurements it is possible to determine the polar and dispersive components of the surface tension as:

$$\gamma_{LV} \cdot (1 + \cos\theta) = 2 \cdot [(\gamma_{LV}^d \cdot \gamma_s^d)^{1/2} + (\gamma_{LV}^p \cdot \gamma_s^p)^{1/2}] \quad (1)$$

where γ_{LV} is the liquid–vapor surface tension, θ is the contact angle, γ_{LV}^d and γ_{LV}^p are the dispersive and polar components of the liquid–vapor interfacial tension, respectively, and γ_s^d and γ_s^p are the dispersive and polar components of the solid surface tension.

Water absorption tests were carried out at 90% RH (simulated from a solution of 34 wt.% of glycerin). Before tests, all the samples were dried under vacuum until constant weight. Samples were weighted at prefixed times and the absorption at each time was calculated as:

$$M_t(\%) = \frac{M_t - M_0}{M_0} \cdot 100 \quad (2)$$

where M_t is the mass of the sample at a time t and M_0 is the initial mass of the sample (dried).

Thermogravimetric analysis (*TGA*) was carried out in a Shimadzu TGA-50 from 30 °C to 1000 °C at 10 °C/min in air and nitrogen. Tests were done for the clay alone, in order to determine the degradation temperature of the organic modifiers, and for nanocomposites to determine the clay content. Using this technique the thermal degradation of the clays in isothermal conditions at temperatures close to those used in the extrusion process (120–140–160–180 °C) for 3 and 30 min was also studied. The maximum heating rate allowed by the equipment was used to reach each temperature. In this case the tests were conducted in air to simulate more realistically the environment during processing operations.

Rheological tests were conducted in a Rheometric Scientific Ares rheometer under nitrogen atmosphere. Plate–plate geometry with a plate diameter of 25 mm was used. Samples were inserted and heated up to 80 °C. Low shear amplitude (2%) was used in order to avoid the destruction of any stabilized clay structure and to work in the lineal viscoelastic regime. Data were taken for shear rates in the range of 0.1–100 s^{-1}.

Tensile tests were performed in a universal testing machine Lloyd Instruments LR30 K at a constant crosshead speed of 50 mm/min. Before tests, all specimens were preconditioned at 65% RH (relative humidity) and room temperature.

Differential scanning calorimetry (*DSC*) tests were performed in a Shimadzu DSC-50 from −105 °C to 100 °C at a heating rate of 10 °C/min under nitrogen atmosphere (ASTM D3417-83). The degree of crystallinity was calculated from the following equation:

$$X_{cr}(\%) = \frac{\Delta H_f}{w_{PCL} \times \Delta H_{100}} \times 100 \quad (3)$$

where ΔH_f is the experimental heat of fusion, w_{PCL} the PCL weight fraction and ΔH_{100} is the heat of fusion of 100% crystalline PCL (136.1 J/g [22]). The glass transition temperature was calculated following the mid-point value procedure of the ASTM D3418-99.

3. Theoretical background

3.1. Rheological characterization

The melt rheology curves were fitted to the power law expression:

$$\eta = A_{Rh} \cdot \dot{\gamma}^{(n_{Rh})} \quad (4)$$

where the *Rh* subscript represents a rheology parameter, η is the dynamic viscosity; A_{Rh} a preexponential factor; $\dot{\gamma}$ the shear rate and n_{Rh} the shear thinning exponent. In the double logarithmic plot a linear zone at low shear rates can be seen. The n_{Rh} parameter was calculated from the slope of this region [23]. Regarding polymer/clay nanocomposites, several authors [23–26] have found that the n_{Rh} value is higher as the clay dispersion degree is improved.

3.2. Young's modulus modeling

3.2.1. Traditional model (Halpin–Tsai)

There are several works in which traditional micromechanical models [27–30] have been employed for the modeling of the tensile modulus of discontinuous reinforcement composites. These kinds of models include various parameters such as the particle volume fraction (f_p), the filler aspect ratio (L/t, where L is the length and t is the thickness of the filler) and orientation (η), and the particle/matrix rigidity ratio (E_p/E_m). Within these models, the Halpin–Tsai equations [29,30] reasonable estimate the stiffness of composites materials, especially for low aspect ratio particles. The model is based on the assumption of perfect polymer/fiber adhesion and randomly distribution of the filler in the whole matrix. It can be expressed by the following equations:

$$\frac{E}{E_m} = \frac{1 + \xi \cdot f_p \cdot \mu}{1 - f_p \cdot \mu} \quad (5a)$$

where

$$\mu = \frac{(E_p/E_m) - 1}{(E_p/E_m) + 2 \cdot (L/t)} \quad (5b)$$

In Eq. (5a) E can represent the longitudinal modulus (E_{11}) or the transverse modulus (E_{33}). For the longitudinal modulus (E_{11}), ξ was given by $2 \cdot (L/t)$. For the transverse modulus E_{33} satisfactory results have been obtained with $\xi = 2$. Besides the aspect ratio and filler modulus, the orientation of the disperse phase has a dramatic effect on modulus [31]. When platelets are randomly oriented, the modulus of the nanocomposite ($E_{3D\text{-rand}}^{platelets}$) should be calculated as:

$$E_{3D\text{-rand}}^{platelets} = 0.49 \cdot E_{11} + 0.51 \cdot E_{33} \quad (6)$$

3.2.2. Effective filler and effective interphase based micromechanical models

The morphology of polymer/layered-silicate nanocomposites has a hierarchical structure. The dispersion of the fillers in a matrix is typically described in terms of exfoliation or intercalation. Fully exfoliated nanocomposites are considered to consist of single clay layers ($t \approx 1$ nm) dispersed in a polymer matrix in which the separation between particles is around 20–50 nm. On the other hand, in the intercalated systems, inter-layer domains of fillers are typically penetrated by polymer chains and consequently stacked with an inter-layer spacing of 1–4 nm. Conventional filler-based micromechanical models previously described by the Halpin–Tsai model do not consider this feature. Thus, a more appropriate model for predicting nanocomposites mechanical properties should include two kinds of descriptors [32]. The primary descriptors are the structural characteristics of the clay related to processing and measured through several parameters such as W_c (clay weight fraction), d_{001} (interlayer spacing), n (number of silicate layers per clay

stack) and the interlayer gallery material. The secondary descriptors are the parameters used in the traditional models; i.e., f_p, L/t and E_p/E_m. Thus, the effective filler parameter should be recalculated before modeling. The idea of effective particle is defined as a well-defined spatial volume occupied by both the silicate layers and the interlayer galleries [31–33]. An intercalated clay particle may be thought as a multi-layer stack containing n single silicate layers (of thickness t_s); thus, the thickness of the effective filler (t_{eff}) may be expressed in terms of the number of platelets per stacked clay (n) and the platelets interlayer spacing (d_{001}) as follows:

$$t_{eff} = (n-1)\cdot d_{001} + t_s \tag{7}$$

From the previous equation it is also possible to obtain other effective parameters: aspect ratio $(L/t)_{eff}$, stiffness (E_p^{eff}) and volume fraction (f_p^{eff}) which are expressed as:

$$(L/t)_{eff} = \frac{L}{t_{eff}} = \frac{L}{(n-1)\cdot d_{001} + t_s} \tag{8a}$$

$$E_p^{eff} = \frac{n\cdot t_s \cdot E_p}{(n-1)\cdot d_{001} + t_s} \tag{8b}$$

$$f_p^{eff} = \frac{W_c\cdot[(n-1)\cdot d_{001} + t_s]}{n\cdot t_s}\cdot\frac{\rho_m}{\rho_p} \tag{8c}$$

where W_c is the weight fraction of clay and ρ_m/ρ_p is the matrix/particle density ratio.

Other authors [34,35] have proposed an effective interphase model to predict the elastic properties of a composite with effective particles having an interphase with the same shape of the effective particle. This zone has a finite size and is related to the matrix/particle interaction zone. It is important to note that overlooking the interphase there is no way to know the influence of the morphological parameters and clay properties related to this zone. A difficulty of this approach is that there is no experimental information about the modulus of interfacial material. Fossey [36] has predicted that the modulus of the interfacial zone (E_I) in nanocomposites is approximately twice of that of the neat polymer (466 MPa in our case). The same author has related the interphase thickness to the polymer radius of gyration, which is 3 nm for PCL. Fertig Iii and Garnich [34] have proposed that the volume fraction of the interphase (V_i) and the matrix (V_m) can be calculated as:

$$V_i = 2\cdot\tau\cdot V_c \tag{9a}$$

$$V_m = 1-(V_c+V_i) = 1-V_c\cdot(1+2\cdot\tau) \tag{9b}$$

where V_c is the clay volume fraction and τ is the ratio between the interphase thickness (3 nm) and the clay thickness (1 nm). This model also considers an *exfoliation factor*, f_e, defined as the quadratic relationship between the planar length of the flake and the width of the periodic unit cell. From all these assumptions, they have derived the constitutive equations for the elastic properties of the nanocomposites generating the coefficients of each equation by means of the use of a finite element model obtaining:

$$\frac{E_{11}}{E_m} - 1 = V_c\cdot\left\{[0.063+0.609\cdot f_e]\cdot\frac{E_p}{E_m} + 2\cdot\tau\cdot[-0.221 + 1.181\cdot f_e]\cdot\frac{E_I}{E_m} + 0557\cdot(1+2\cdot\tau)\right\} \tag{10a}$$

$$\frac{E_{33}}{E_m} - 1 = V_c\cdot\left\{[-1.1+2.457\cdot f_e]\cdot\ln\left(\frac{E_p}{E_m}\right) + [3.659-3.540\cdot f_e]\cdot\ln\left(\frac{E_I}{E_m}\right) + 0.329\cdot(1+2\cdot\tau)\right\} \tag{10b}$$

Table 2
Results of contact angle tests of several commercial clays.

Clay	Contact angle		
	Ethylene glycol (polar)	Water (higly polar)	CH_2I_2 (non-polar)
C30B	–	43.42 ± 0.11	–
C10A	49.35 ± 0.67	–	37.03 ± 0.57
C93A	45.39 ± 0.36	45.58 ± 1.22	38.17 ± 0.29
C20A	62.39 ± 0.49	52.13 ± 0.37	40.53 ± 0.67

4. Results and discussion

4.1. Characterization of clays

The interlaminar space ($d_{001}^{initial}$) of the nanoclays (Table 1) was verified by XRD tests. This parameter is important because it is expected that as $d_{001}^{initial}$ increases, polymer chains have more space to intercalate, obtaining a better dispersed nanocomposite. The highest values were found for the clays C93A and C20A.

Another main factor is the polarity of the filler, due to the fact that the matrix is hydrophobic with a very low degree of polarity; around 6% [37], its interaction will be higher with the less hydrophilic filler. The results of contact angle tests are summarized in Table 2. The lower values of surface polarity of the clays were obtained with C10A and C20A. The results for CNa+ and C25A are not shown because it was not possible to obtain stable droplets of different solvents on the surface of the clay tablets. Besides the superficial analysis, the degree of polarity of the clays was also compared by moisture absorption tests, which provides information about the overall performance of the material. Fig. 1a and b shows the results of water absorption as a function of time and after 24 h, respectively. The C93A and C20A clays had the lowest water absorption values. After determining the basal spacing of clays and the filler/matrix compatibility, C20A and C93A clays seem to be the best candidates for the preparation of nanocomposites with PCL as matrix, taking into account the hydrophobic nature of this polymer.

As it was previously explained in the introduction, the thermal and mechanical stability of the organic-modifiers of the clays can be decisive to obtain the expected clay morphology when the nanocomposites are prepared by means of intense shear and temperature as those involved in a twin-screw extruder [38]. Fig. 2a and b shows the residual mass of clay as a function of temperature and the DTGA analysis, respectively. The peaks of the latter indicate the maximum speed of thermal degradation. It can be observed from Fig. 2a that the clay CNa+ has a steep drop in residual mass in the range of 50–120 °C due to evaporation of water from the sample, showing that this reinforcement is the one with greater hydrophilic character (as was also shown from Fig. 1). Table 3 summarizes the water content (calculated as the mass loss at 120 °C), the content of organic modifier within each clay (calculated as the mass loss at 900 °C by subtracting the appropriate water content) and the temperature for the maximum degradation rate (T_{peak}) of the clay modifiers. As was expected, the most hydrophilic clay (CNa+, unmodified) showed the highest values of water absorption and

Table 3
Results of dynamic thermogravimetric analysis (TGA, DTGA).

Clay	Water content (wt.%)	Modifier content (wt.%)	T_{peak} (°C)
CNa+	9.9	–	–
C25A	1.4	33	300
C30B	2.2	28	268
C10A	1.6	41	235
C93A	0.6	38	338
C20A	1.8	40	304

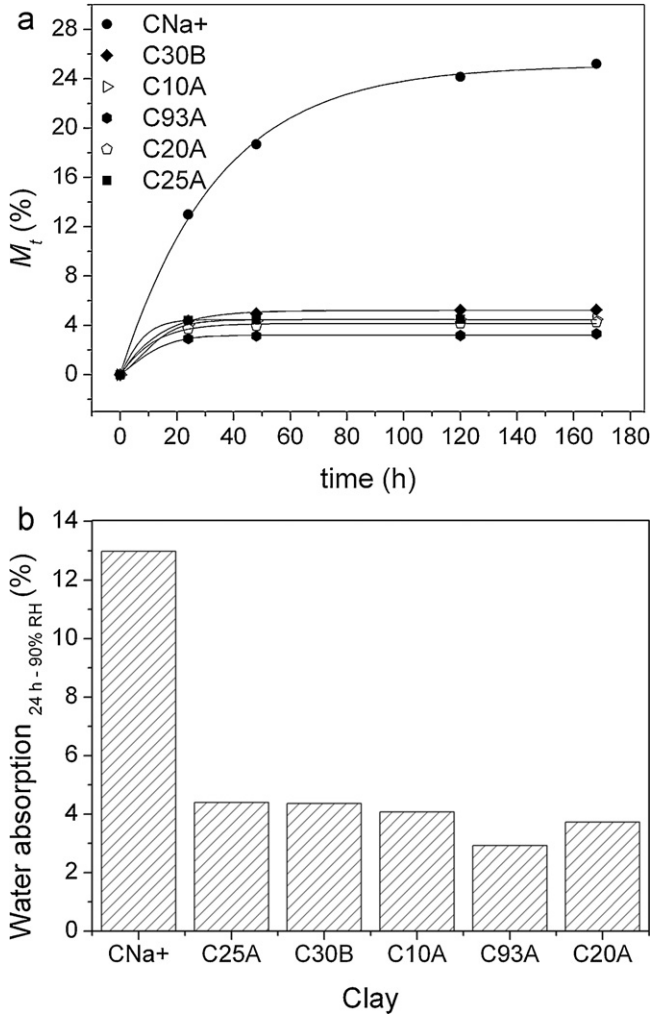

Fig. 1. (a) Water absorption of different clays as a function of time. (b) Water absorption of different clays after 24 h.

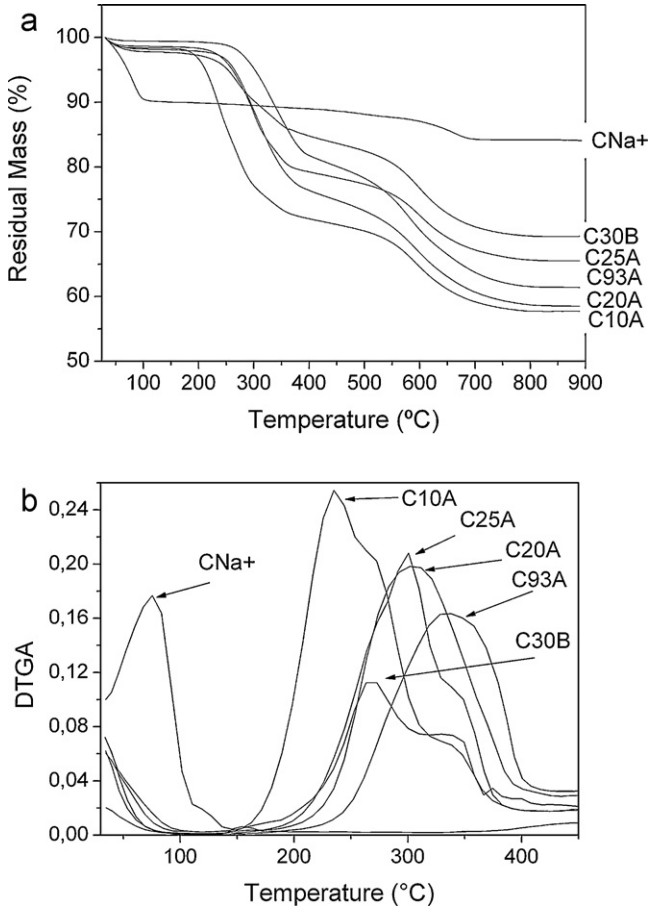

Fig. 2. (a) Residual mass of the clays as a function of temperature (TGA). (b) Derivative of the residual mass of the clays (DTGA) as a function of temperature.

water content (TGA), while the lowest values of both tests were obtained with C93A.

It can be observed from Table 3 that the degradation temperatures of the organic modifiers were in the range of 235–338 °C (the limits for C10A and C93A, respectively). The same table shows that the amount of modifier cation on the total mass of clay is high (between 28% and 41% by weight), therefore, it is crucial to consider their degradation during processing because if it happens, not only the final dispersion degree of the clay can be affected, but also the final clay content inside the matrix will be lower than that introduced in the extruded if silicate layers and organic modifiers are considered as an individual particle. In our case, the processing temperature on the extruder barrel did not exceed 120 °C, but it is well known that the shear forces developed in the mixer, together with the high viscosity of the polymer, cause an increase in the melt temperature by viscous dissipation; therefore, the clay modifiers may have degraded in different proportions, both thermal and mechanically, depending on the characteristics of each one.

Dynamic TGA analysis was a tool to demonstrate that the possibility of degradation of the clay organic modifiers during extrusion is a real fact. In order to simulate the real conditions of the mixing process in a better way (fixed temperature and air atmosphere during the residence time of the polymer/clay mixture inside the extruder), isothermal TGA tests at different temperatures in air atmosphere were performed in the range of 120–180 °C, which are the usual temperatures to process PCL and several traditional polymers. Fig. 3a–c shows the weight loss for each clay obtained from the isothermal TGA tests at 120 °C and 180 °C for 3 and 30 min of residence time. It was assumed, based on dynamic tests of TGA (Fig. 2a), that even at the lower temperature analyzed (120 °C) all the water is extracted from the sample. In order to analyze events only related to organic modifiers, the water content of each clay (Table 3) was subtracted to the values of weight loss. The residence times of 3 and 30 min were selected since the first value is close that used to prepare the samples and the second is an extreme condition that would allow us to quantify significant results. Weight loss was not observed at 120 °C in any case. With this result we conclude that at this temperature only water extraction is taking place. Fig. 3a compares the results between the unmodified clay (CNa+) and the modified with lower thermal stability (C10A). As expected, in the case of CNa+ weight loss was not observed in the range of times and temperatures analyzed because it is not chemically modified. On the other hand, analyzing the results at 180 °C for C10A, we observed that weight loss at 30 min was 9 times higher than at 3 min which can be attributed to thermal degradation of the organic modifier. The same trend was obtained by comparing the values at 180 °C for 3 and 30 min for all modified clays, except for C20A. It must be emphasized the importance of this result as 180 °C is a temperature 50 °C below the lower temperature of degradation calculated from the dynamic tests (Fig. 2b), and it is within the range of processing temperatures of the PCL and traditional engineering polymers. While 30 min is a value that is well above the residence time at which a polymer is usually submitted in an extruder, one should not forget that the isothermal TGA tests do

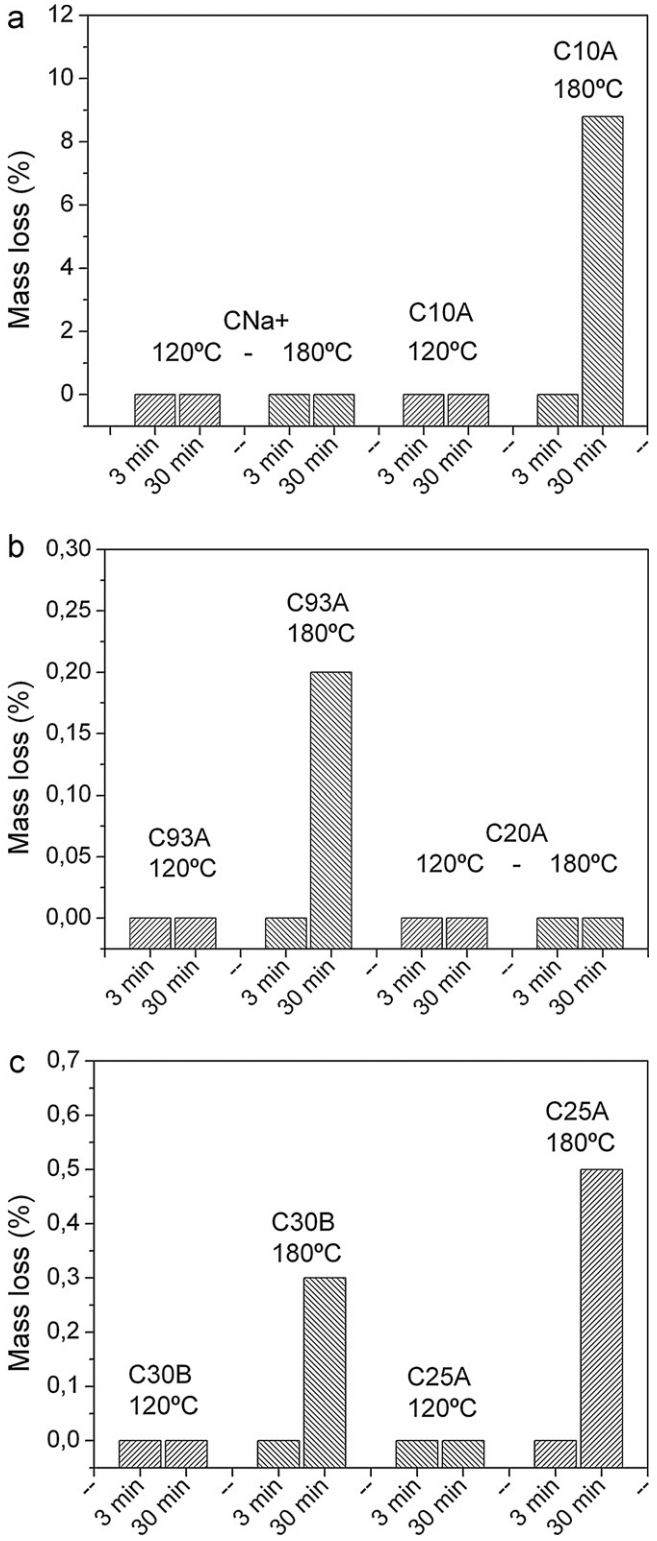

Fig. 3. (a) Mass loss at 120 °C and 180 °C (3 and 30 min) for CNa+ and C10A (TGA). (b) Mass loss at 120 °C and 180 °C (3 and 30 min) for C93A and C20A (TGA). (c) Mass loss at 120 °C and 180 °C (3 and 30 min) for C30B and C25A (TGA).

not simulate shear forces, which not only increase melt temperature by viscous dissipation, but also can mechanically degrade the organic modifiers, which can promote their degradation even at lower processing temperatures and/or lower residence times. This can lead to a material with different properties from those expected when the preparation of the nanocomposite is only focused in optimizing the matrix/reinforcement compatibility. In order to complete this analysis, the authors of this work are currently studying how to incorporate the shear stresses in the thermal degradation tests.

Table 4
Results of XRD and melt rheology for nanocomposites based on PCL and 5 wt.% of several clays.

Material	$-n_{Rh}$	d_{001}^{final} (Å)	Δd_{001} (%)
PCL/CNa+	0.06	14.1	21
PCL/C25A	0.35	28.3	52
PCL/C30B	0.32	33.1	79
PCL/C10A	0.19	28.3	47
PCL/C93A	0.28	28.9	22
PCL/C20A	0.39	–	–

4.2. Characterization of nanocomposites

The final properties of nanocomposites are determined by both the reinforcement content and the degree of dispersion of it into the matrix [3]. It was determined by TGA tests that the clay weight content inside the nanocomposites was in the range of 5.0 ± 0.6 wt.%. These calculations were carried out taking into account that neither mechanical nor thermal degradation of the clay organo-modifiers took place during the intercalation process in order to ensure that the clay content introduced in the extruder was maintained and because in case organo-modifiers degradation took place it is not possible to accurately quantify it.

The morphology of the nanocomposites was analyzed by means of the interlayer spacing of the clay inside the nanocomposites (d_{001}^{final}), the increment in the interlayer distance ($\Delta d_{001} = ((d_{001}^{final} - d_{001}^{initial})/d_{001}^{initial}) \times 100$) and the shear thinning exponent (n_{Rh}). The values are shown in Table 4. As was expected, all nanocomposites prepared with organo-modified clays showed higher Δd_{001} and d_{001}^{final} values than PCL/CNa+. This result is an indicator of the higher dispersion degree of the filler inside the matrix, which is a direct consequence of the enhanced polymer/clay compatibility. Moreover, the PCL/C30B nanocomposite showed the highest values of these parameters. The PCL/C20A nanocomposite was the only case in which the d_{001}^{final} value could not be calculated due to the disappearance of the diffraction peak (Fig. 4). There are two possible reasons for this behavior, the structure of the nanocomposite is intercalated but the value of d_{001}^{final} is so high that it could not be calculated by means of the equipment used, or the nanocomposite does not present ordering anymore (exfoliated structure). Whatever the reason, it can be ensure that the C20A clay

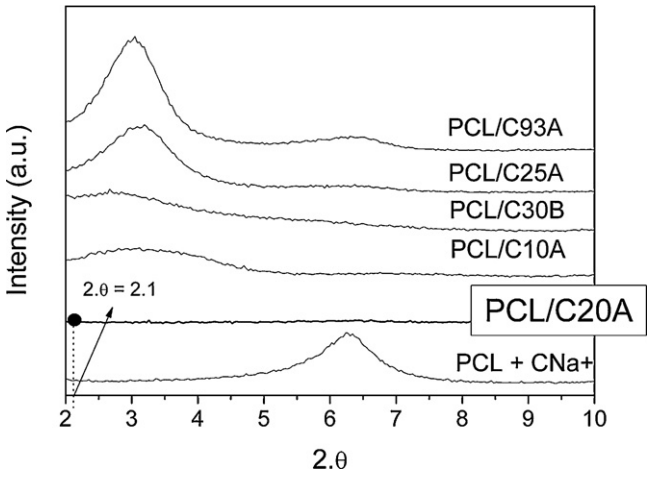

Fig. 4. XRD patterns of the studied nanocomposites.

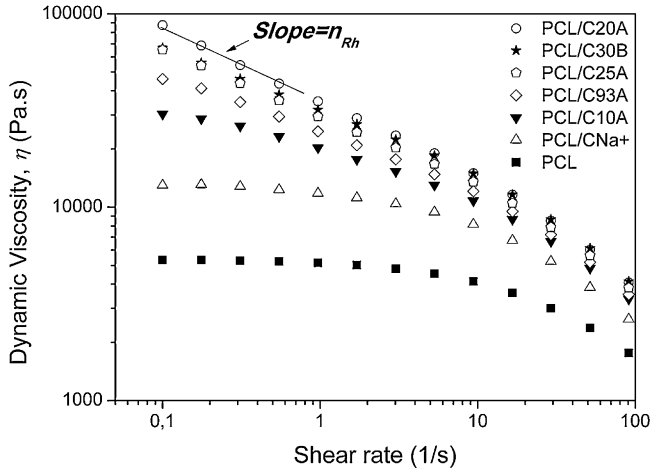

Fig. 5. Dynamic viscosity, η, as a function of shear rate for PCL and nanocomposites: points are experimental values and the line represents the power law fitting.

would have shown the highest d_{001}^{final} value. On the other hand, we calculated what should be the position of the 2θ diffraction peak of PCL/C20A for the highest value of Δd_{001} obtained, which corresponds to the PCL/C30B nanocomposite (Table 4). The result was $2\theta = 2.1^{\circ}$ but it can be seen in Fig. 4 that no peak is present for PCL/C20A at that position, marked with a black dot in the figure, which suggests that the value of Δd_{001} was even greater than that of the PCL/C30B and that the PCL/C20A showed the highest degree of dispersion of the clay within the matrix.

Fig. 5 shows the dynamic viscosity, η, as a function of the shear rate, $\dot{\gamma}$, for the matrix and nanocomposites. PCL and PCL/CNa+ showed a Newtonian behavior at low shear rate, with higher viscosity for PCL/CNa+ as a result of the impedance of the polymer chains to flow around the rigid MMT particles, while the nanocomposites prepared with the organo-modified clays showed a pseudo-solid-like behavior with pronounced shear thinning (higher n_{Rh}, Table 4). It is clear the tendency of higher n_{Rh} for the nanocomposites with the best clay dispersion degree (PCL/C20A, PCL/C30B), while the lowest value was obtained with the worst dispersed nanocomposite (PCL/CNa+). The same trend was found by other authors [23–26] for similar thermoplastic/clay systems.

Even when all nanocomposites prepared with organo-modified clays showed higher clay dispersion degree than the PCL/CNa+, by comparing the compatibility between the matrix and the reinforcement to the degree of dispersion of the clay within the matrix, the C20A clay is the only one that presented consistent results (the higher the compatibility, higher degree of dispersion of the clay in the nanocomposite). The C20A organo-modifier showed the highest thermal resistance, which suggests that the degradation kinetic of the organic modifiers and the kinetic of their interaction with the polymer chains are as influential on the final dispersion degree of reinforcement in the matrix as the compatibility between the components. It must be taken into account that these results will determine the final properties of the nanocomposite.

The mechanical properties of the PCL and its nanocomposites are summarized in Table 5.

As a general result, it was observed that all clays enhance the Young's modulus of the neat matrix, while the tensile strength remained almost constant and the elongation at break decreased 36% in most cases. Fig. 6 shows a plot of the relative Young's modulus (E_{nc}/E_m) as a function of the clay dispersion degree, the latter by means of the d_{001}^{final} parameter. The value of d_{001}^{final} for PCL/C20A was calculated on the basis of the highest Δd_{001} obtained ($\Delta d_{001} = 79\%$ for PCL/C30B). In the same figure, a descendent ranking for polymer/clay compatibility constructed from the water adsorption and

Table 5
Mechanical properties for the PCL and its nanocomposites.

Material	Modulus (MPa)	E_{nc}/E_m [a]	Strength (MPa)	Elongation at break (%)
PCL	233 ± 7	1	15.0 ± 0.3	1906 ± 82
PCL/CNa+	240 ± 8	1.03	15.8 ± 1.3	1345 ± 123
PCL/C25A	253 ± 13	1.09	14.3 ± 0.6	1553 ± 119
PCL/C30B	303 ± 28	1.30	14.0 ± 0.2	1212 ± 38
PCL/C10A	250 ± 27	1.07	14.7 ± 0.6	1274 ± 134
PCL/C93A	250 ± 26	1.07	14.6 ± 0.4	1534 ± 29
PCL/C20A	331 ± 30	1.42	14.1 ± 0.9	1430 ± 35

[a] E_{nc} and E_m are Young's modulus of nanocomposite and matrix, respectively.

contact angle tests is also shown. From this figure it is clear that the enhancement of the relative Young's modulus is a function of the clay dispersion degree, as was widely demonstrated in the literature and reviewed by Alexandre and Dubois [21]. Even so, the tendencies between PCL/C10A, PCL/C25A and PCL/C93A are not so evident. Moreover, if we analyze the polymer/clay compatibility, no explainable tendency on the Young's modulus can be built up. We attributed this result to the degradation of the organic-modifiers since the clays used to prepare PCL/C10A, PCL/C25A and PCL/C93A nanocomposites are those that showed the lowest thermal stability, as was demonstrated by isothermal TGA analysis in Fig. 3a–c. Therefore, the degradation of the organic modifier will not only affect the intercalation process and the final clay dispersion degree; but also will modify the final clay content inside the matrix which are the main parameters responsible on the final relative Young's modulus of the nanocomposite [1,3,21,39]. The degree of crystallinity (X_{cr}) and glass transition temperature (T_g) of the matrix are properties that also influence the mechanical properties of the material. It has been observed [40–44] that clays may have no effect as well as lead to decreases or increases in the values of these properties and melting temperature (T_m) of different matrices. Therefore, this analysis is required for each particular polymer/clay system including the type of processing used. Table 6 shows the thermal properties for the PCL and its nanocomposites. For each material, the dispersion in values was negligible (less than 1%). A slight decrease in the degree of crystallinity was observed when the clay was incorporated to the matrix but no clear trend was found. Even so, the differences between each material are very small and can

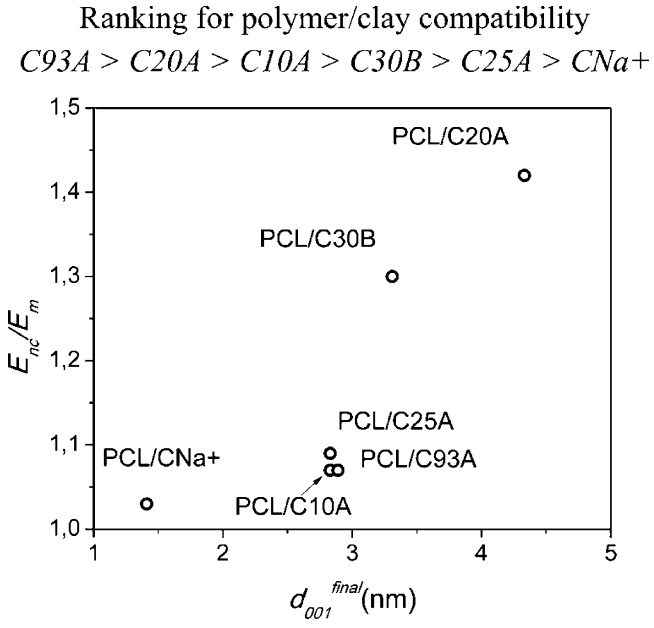

Fig. 6. Relative Young's modulus as a function of the clay dispersion degree (d_{001}^{final}).

Table 6
Thermal properties of PCL and its nanocomposites.

Material	X_{cr} (%)	T_m (°C)	T_g (°C)
PCL	72	66	−63
PCL/CNa+	68	65	−64
PCL/C25A	71	65	−63
PCL/C30B	72	64	−63
PCL/C10A	68	65	−63
PCL/C93A	69	65	−63
PCL/C20A	71	64	−63

be attributed to experimental errors. Labidi et al. [44] found similar results for the PCL reinforced with three different modified clays. On the other hand, no significant changes were observed in the melting temperature or glass transition temperature between the different materials. The same behavior was observed by Marras et al. [43] for PCL nanocomposites with different amounts of C25A. Therefore, it can be thought that the thermal properties did not have influence on the tendencies observed for the relative Young's modulus.

Another way to study the effectiveness of the clay enhancing the rigidity of the matrix, is analyzing theoretical parameters related to the degree of dispersion of the clay calculated from the effective filler and effective interphase based micromechanical models. The theoretical n value was calculated by the combination of Eq. (6) with Eqs. (5a and b) and (8a–c). In this way the only unknown parameter of the model is n since $E_{3D\text{-rand}}^{platelets}$ is the experimental Young's modulus of the nanocomposites, $d_{001} = d_{001}^{initial}$ and ρ_p are reported in Table 1, $\rho_m = 1.2\,g/cm^3$ and $t_s = 1\,nm$, $L = 100\,nm$ and $E_p = 175\,GPa$ were reported by Dai et al. for MMT silicate layers [45]. These parameters were also used to calculate f_e by the combination of Eq. (6) with Eqs. (5a and b) and (10a and b). Table 7 shows the relative n values ($n_r = n/n_{max}$, where n_{max} is the maximum value of n) and the theoretical f_e values. Analyzing the previous table, it can be observed that the effective filler modulus decreases as the value of $d_{001}^{initial}$ increases. This observation is very important for the prediction of the intercalated nanocomposites modulus and is not considered in the traditional micro-mechanical models in which the reinforcing particle is considered to be an individual silicate layer of thickness $t_s < t_{eff}$ and Young's modulus of $E_p > E_p^{eff}$. For some clays (CNa+, C25A, C10A and C93A), the exfoliation factor was equal to 0 which would mean that there is no exfoliated regions in the nanocomposite and could be related to a low dispersion degree of the clay. Fig. 7a–c shows the relationships between the different parameters analyzed. Fig. 7a shows that there is no clear trend between f_e and n_r. High n_r values are not always related to poor dispersion degree of the clay since stacked particulates having high d_{001} values can be considered as exfoliated regions [21]. This analysis is represented by the behavior of the nanocomposites with CNa+ and C20A, since the former showed the lower n_r value and lower degree of dispersion and the second presented high n value and greater dispersion. On the other hand, Fig. 7b and c shows that the materials with $f_e = 0$ are those with the lowest Δd_{001} and d_{001}^{final} values. The last two parameters are related with the degree

Table 7
Young's modulus modeling of the nanocomposites.

Material	f'_p	E_p^{eff} [a] (GPa)	f_p^{eff} [b]	n_r	f_e (%)
PCL/CNa+	0.11	155.0	0.029	1	0.0
PCL/C25A	0.08	100.6	0.044	9	0.0
PCL/C30B	0.08	97.1	0.036	1	2.6
PCL/C10A	0.08	95.4	0.015	2	0.0
PCL/C93A	0.08	76.7	0.038	7	0.0
PCL/C20A	0.07	75.2	0.085	4	1.8

[a] Eq (8b).
[b] Eq. (8c).

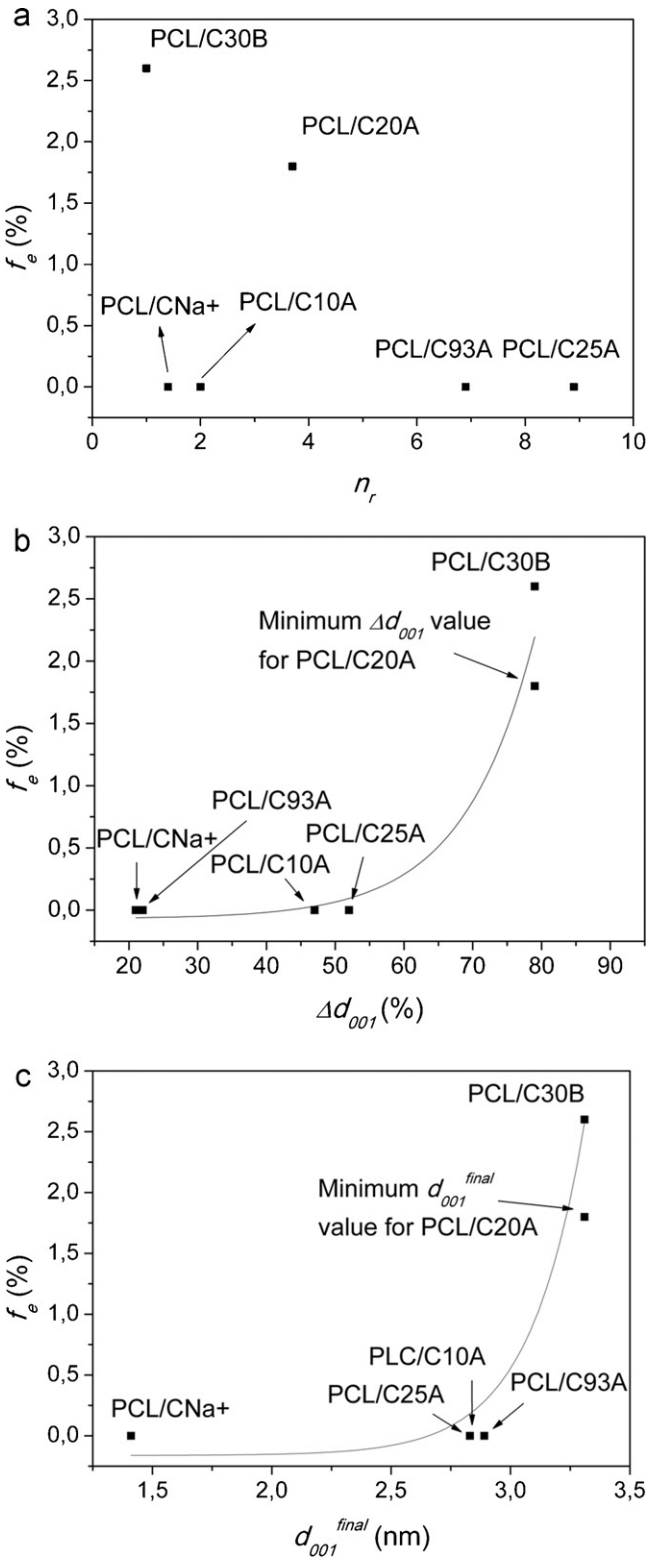

Fig. 7. (a) Theoretical parameters from Young's modules modeling, f_e as a function of n_r. (b) Theoretical parameters from Young's modules modeling, f_e as a function of Δd_{001}. (c) Theoretical parameters from Young's modules modeling, f_e as a function of d_{001}^{final}.

of dispersion of the reinforcement within the matrix, therefore it suggests that f_e better represents the morphology of the nanocomposites than n_r. This conclusion is interesting as an additional tool to compare the morphology of different polymer/clay nanocomposites when TEM observations are not reliable and experimental Young's modulus and d_{001}^{final} values of the nanocomposites are available.

5. Conclusions

The Young's modulus of polymer clay nanocomposites depends on both the clay dispersion degree and the clay content inside the matrix. It was shown that organo-modified clays improve the effectiveness enhancing the rigidity of the matrix. This result was a consequence of the higher dispersion degree of the clay but it was not found a clear trend related to the polymer/clay compatibility which was attributed to the degradation of clay organo-modifiers during processing. The C20A clay showed the highest thermal stability and good compatibility with PCL which led to the nanocomposite with the highest clay dispersion degree and hence optimal mechanical performance. The theoretical parameters describing the clay dispersion degree that were obtained from the effective micro-mechanical modeling supported these results. The following studies will be performed only for the PCL and the nanocomposites with C20A, C30B (which showed the best performance) and CNa+ (used as reference).

As a general conclusion, when polymer/organo-modified clay nanocomposites are prepared by techniques such as extrusion, in which temperature and shear forces are involved, the degradation of the clay organo-modifiers can take place. In this case, improving polymer–clay compatibility may not be the main factor to achieve the best mechanical performance.

Acknowledgements

Authors acknowledge to Mincyt, UNMdP and CONICET for the financial support.

References

[1] B. Lepoittevin, M. Devalckenaere, N. Pantoustier, M. Alexandre, D. Kubies, C. Calberg, R. Jérôme, P. Dubois, Polymer 43 (2002) 4017–4023.
[2] M. Kunioka, F. Ninomiya, M. Funabashi, Polymer Degradation and Stability 92 (2007) 1279–1288.
[3] L.N. Ludueña, V.A. Alvarez, A. Vazquez, Materials Science and Engineering: A 460–461 (2007) 121–129.
[4] P.B. Messersmith, E.P. Giannelis, Journal of Polymer Science Part A: Polymer Chemistry 33 (1995) 1047–1057.
[5] Y. Kojima, A. Usuki, M. Kawasumi, A. Okada, Y. Fukushima, T. Kurauchi, O. Kamigaito, Journal of Materials Research 8 (1993) 1185–1189.
[6] J.W. Gilman, C.L. Jackson, A.B. Morgan, R. Harris, E. Manias, E.P. Giannelis, M. Wuthenow, D. Hilton, S.H. Phillips, Chemistry of Materials 12 (2000) 1866–1873.
[7] G. Gorrasi, M. Tortora, V. Vittoria, E. Pollet, B. Lepoittevin, M. Alexandre, P. Dubois, Polymer 44 (2003) 2271–2279.
[8] Z. Zhang, J.-L. Yang, K. Friedrich, Polymer 45 (2004) 3481–3485.
[9] P. Maiti, Langmuir 19 (2003) 5502–5510.
[10] W. Xie, Z. Gao, W.P. Pan, D. Hunter, A. Singh, R. Vaia, Chemistry of Materials 13 (2001) 2979–2990.
[11] W. Xie, Z. Gao, K. Liu, W.P. Pan, R. Vaia, D. Hunter, A. Singh, Thermochimica Acta 367–368 (2001) 339–350.
[12] D.L. VanderHart, A. Asano, J.W. Gilman, Macromolecules 34 (2001) 3819–3822.
[13] D.L. VanderHart, A. Asano, J.W. Gilman, Chemistry of Materials 13 (2001) 3796–3809.
[14] P.J. Yoon, D.L. Hunter, D.R. Paul, Polymer 44 (2003) 5341–5354.
[15] T.D. Fornes, P.J. Yoon, H. Keskkula, D.R. Paul, Polymer 42 (2001) 9929–9940.
[16] T.D. Fornes, P.J. Yoon, H. Keskkula, D.R. Paul, Polymer 43 (2002) 2121.
[17] R. Krishnamoorti, R.A. Vaia, E.P. Giannelis, Chemistry of Materials 8 (1996) 1728–1734.
[18] J.W. Cho, D.R. Paul, Polymer 42 (2001) 1083–1094.
[19] R. Krishnamoorti, K. Yurekli, Current Opinion in Colloid and Interface Science 6 (2001) 464–470.
[20] J.C. Matayabas Jr., S.R. Turner, Polymer–Clay Nanocomposites, Wiley, New York, 2000.
[21] M. Alexandre, P. Dubois, Materials Science and Engineering R: Reports 28 (2000) 1–63.
[22] W.Y. Yam, J. Ismail, H.W. Kammer, H. Schmidt, C. Kummerlöwe, Polymer 40 (1999) 5545–5552.
[23] R. Wagener, T.J.G. Reisinger, Polymer 44 (2003) 7513–7518.
[24] J. Zhao, A.B. Morgan, J.D. Harris, Polymer 46 (2005) 8641–8660.
[25] R. Krishnamoorti, J. Ren, A.S. Silva, Journal of Chemical Physics 114 (2001) 4968–4973.
[26] A. Durmus, A. Kasgoz, C.W. Macosko, Polymer 48 (2007) 4492–4502.
[27] J.D. Eshelby, Proceedings of the Royal Society of London. Series A. Mathematical and Physical Sciences 241 (1957) 376–396.
[28] R. Hill, Journal of the Mechanics and Physics of Solids 13 (1965) 213–222.
[29] J.C. Halpin, Journal of Composite Materials 3 (1969) 732–734.
[30] J.C. Halpin, J.L. Kardos, Polymer Engineering and Science 16 (1976) 344–352.
[31] T.D. Fornes, D.R. Paul, Polymer 44 (2003) 4993–5013.
[32] N. Sheng, M.C. Boyce, D.M. Parks, G.C. Rutledge, J.I. Abes, R.E. Cohen, Polymer 45 (2004) 487–506.
[33] J.I. Weon, H.J. Sue, Polymer 46 (2005) 6325–6334.
[34] R.S. Fertig Iii, M.R. Garnich, Composites Science and Technology 64 (2004) 2577–2588.
[35] G.M. Odegard, T.C. Clancy, T.S. Gates, Polymer 46 (2005) 553–562.
[36] S. Fossey, Executive Conference Managment, San Diego, California, 2002.
[37] V. Alvarez, I. Mondragón, A. Vázquez, Composite Interfaces 14 (2007) 605–616.
[38] S. Su, C.A. Wilkie, Polymer Degradation and Stability 83 (2004) 347–362.
[39] Y. Di, S. Iannace, E. Di Maio, L. Nicolais, Journal of Polymer Science, Part B: Polymer Physics 41 (2003) 670–678.
[40] P. Rittigstein, J.M. Torkelson, Journal of Polymer Science, Part B: Polymer Physics 44 (2006) 2935–2943.
[41] J.L. Keddie, R.A.L. Jones, R.A. Cory, Faraday Discussions 98 (1994) 219–230.
[42] K. Masenelli-Varlot, E. Reynaud, G. Vigier, J. Varlet, Journal of Polymer Science, Part B: Polymer Physics 40 (2002) 272–283.
[43] S.I. Marras, K.P. Kladi, I. Tsivintzelis, I. Zuburtikudis, C. Panayiotou, Acta Biomaterialia 4 (2008) 756–765.
[44] S. Labidi, N. Azema, D. Perrin, J.-M. Lopez-Cuesta, Polymer Degradation and Stability 95 (2010) 382–388.
[45] Y. Dai, Y.-W. Mai, X. Ji, Composites Part B: Engineering 39 (2008) 1062–1068.